ELSEVIER

In Collaboration with
the Netherlands Institute for Sea Research

JOURNAL OF SEA RESEARCH

Journal of Sea Research 38 (1997) 173–193

The primary production module in the marine ecosystem model ERSEM II, with emphasis on the light forcing

W. Ebenhöh [a,*], J.G. Baretta-Bekker [b], J.W. Baretta [b]

[a] *Carl von Ossietzky Universität, Postfach 2503, D-26111 Oldenburg, Germany*
[b] *Ecological Modelling Centre, Joint department of Danish Hydraulic Institute and VKI, Agern Allé 5, DK-2970 Hørsholm, Denmark*

Received 3 October 1996; accepted 8 July 1997

Abstract

New elements in the primary production module of ERSEM II relative to ERSEM I are described. The main changes are the inclusion of picoalgae and dinoflagellates as additional functional groups, the decoupling of carbon- and nutrient-uptake kinetics and the refining of the light dependency of the primary producers, with emphasis on the last. The results of a reference run are compared with measurements. The consequences of using production-irradiance (p/I) relations assuming a different degree of photoinhibition in calculating net annual primary production are shown in a sensitivity analysis, and it is concluded that a p/I relation with a high degree of photoinhibition leads to clear underestimates of primary production in turbid coastal waters.

Keywords: ecosystem model; p/I curves; irradiance; primary production; ERSEM

1. Introduction

The primary production module described here is part of the European Regional Seas Model-II. ERSEM II is the successor to ERSEM I (Baretta et al., 1995), which in turn was a further development of estuarine ecosystem models, as described in Baretta and Ruardij (1988) and Anonymous (1988). ERSEM comprises a number of submodels and modules, each describing a number of state variables, with the interactions between the state variables from the different submodels defining the emergent dynamics of the whole system by running the whole set of submodels together in a simulation framework (Ruardij et al., 1995).

The integration of so many processes in one model was possible by the modular setup of the model, with each of the participating institutes being responsible for the development and testing of one submodel in the framework of a standard version of the model (Blackford and Radford, 1995).

Concerning the primary production module the objective was to disaggregate and refine the primary production module of ERSEM I (Varela et al., 1995). This has been done by: (1) including picoalgae and dinoflagellates as additional functional groups in the phytoplankton; (2) refining the calculation of the underwater light climate and its effect on primary production at the chosen vertical resolution; and (3) incorporating nutrient uptake kinetics according to Droop (1974) and Nyholm (1977).

Picoalgae and dinoflagellates were introduced to have a better resolution of the size spectrum of the

* Corresponding author. Tel.: +49 (441) 9706 344; Fax: +49 (441) 7983 404; E-mail: w.ebenhoeh@icbm.uni-oldenburg.de

1385-1101/97/$17.00
PII S1385-1101(97)00043-9

primary producers. On the one hand this allows a more precise definition of the growth characteristics of the primary producers and on the other hand it permits refining the grazing interactions in the microbial food web (Baretta-Bekker et al., 1998).

The reason for refining the treatment of the underwater light climate and its expression in a dimensionless light-limitation factor was that the use of Steele's p/I function (Steele, 1974) in combination with the high level of extinction in the turbid coastal boxes and the coarse vertical resolution of the model caused severe overestimates of the light limitation. Steele's formula assumes photoinhibition to suppress primary production strongly above the depth of photoadaptation, irrespective to the duration of exposure to above-optimal irradiance levels. McGillicuddy (1995) analysed the consequences of the relationship between the photoadaptive response and the rate of vertical mixing. He concludes that the apparent discrepancy between results obtained using a Lagrangian integration and a Eulerian integration is a result of different parameterisations of photoadaptive reaction kinetics (and consequently of photoinhibition).

Including nutrient uptake kinetics in fact decouples carbon assimilation and nutrient uptake dynamics, with potentially far-reaching consequences for the functioning of the microbial food web as this decoupling allows the excretion by primary producers of DOM in the form of carbohydrates. In situations where these nutrient-deficient substances predominate in the dissolved organic carbon (DOC) pool, bacterioplankton tend to become nutrient-limited instead of substrate-limited and compete directly with phytoplankton for inorganic nutrients (Bratbak and Thingstad, 1985). The outcome of this competition depends on the trophic interactions in the microbial food web between bacterioplankton, heterotrophic nanoflagellates, microzooplankton and mesozooplankton (Baretta-Bekker et al., 1994, 1995, 1997, 1998). This can explain where, when and why differently structured food webs (Legendre and Rassoulzadegan, 1995) may be expected to occur, as well as why DOC may accumulate in oligotrophic systems (Thingstad and Rassoulzadegan, 1995).

This paper concentrates on the various aspects of the effect of the underwater light climate, while the effects of the decoupled carbon and nutrient dynamics are described in Baretta-Bekker et al. (1997).

2. The primary producer module in general

The primary producers in the model consist of four functionally different groups, which are operationally defined as:

- picoalgae, phytoplankton in the size class 0.2 to 2 μm equivalent spherical diameter (ESD), eaten by heterotrophic nanoflagellates;
- autotrophic flagellates, from 2 to 20 μm ESD, eaten by heterotrophic nanoflagellates, micro- and mesozooplankton;
- diatoms, from 20 to 200 μm ESD, eaten by micro- and mesozooplankton;
- dinoflagellates, from 20 to 200 μm ESD, not grazed in the model.

All groups are modelled in the same way, hence, only one standard primary producer, called P, is described in the following part. The groups differ in their parametrisation only, with the exception of the silicate dependence of diatoms.

The standing stocks are described as densities of the carbon-, nitrogen-, phosphorus- and, in the case of diatoms, silicate-components of the biomass: P_c, P_n, P_p, P_s. Carbon is expressed in mg C m^{-3}, while the nutrients are expressed in mmol m^{-3}. The carbon uptake by assimilation and the loss processes, respiration, excretion and lysis, are functions of the intracellular nutrient quota $k_n = P_n/P_c$ for nitrogen and $k_p = P_p/P_c$ for phosphorus. The nutrient uptake processes (from NH_4, NO_3 and PO_4) are decoupled from the carbon assimilation process. Nutrient uptake is dependent on the external nutrient concentrations and on the level of the intracellular nutrient storage. For the silicate uptake (diatoms only) no internal storage is assumed, hence, carbon assimilation of diatoms is additionally dependent on the external SiO_4-concentration, and the Si-uptake is proportional to carbon assimilation.

In the case of negative net production (respiration exceeds production, e.g. in winter and in deeper water layers) nutrient release may occur. All processes are temperature dependent with the same Q_{10} value.

The light dependence of carbon assimilation is complex. The phytoplankton community is not completely characterised by the biomass values of the

four groups in the boxes, but additionally photoadaptation in the form of an optimal light variable I_{opt} is introduced. This dynamic variable tracks the light history, making the phytoplankton less dependent on seasonally and spatially varying light conditions than would be the case with fixed optimal light parameters, as the phytoplankton now adapts to seasonal variations and to some extent to day-to-day variations in the underwater light climate.

3. Light dependence of primary production

Irradiance is determined by known laws of physics until it reaches the phytoplankton cell. Then biology takes over. The uncertainties in production are predominantly due to the biological regulation processes. The precision of the physical calculations of the light is not very helpful because the remaining biological uncertainty is large. In ERSEM a quite complicated theory forms the base for the light submodule, extending earlier work by others (Nyholm, 1978; Tett et al., 1986; Taylor and Joint, 1990). However, it will be shown that the depth-integrated effect of irradiance on the primary production in the water column mainly depends on two factors: daylength and extinction coefficient. These two factors have also been shown by Behrenfeld and Falkowski (1997) as to explain much of the variability in observed vertical distribution of daily primary production. All other factors are of secondary importance. If this analysis is correct one has to ask, why such a complicated theory in the model instead of forcing the model with just these two factors? There is, however, another aspect: there certainly is some merit in speculating on how biological mechanisms (such as storage/conversion of light energy) may affect the utilisation of light under water and how this would modify the formulation of appropriate algorithms expressing this relationship in box models.

The physical processes that are taken into account in defining the light forcing of primary productivity in the model, are well studied and described partly empirically (Dobson and Smith, 1988). These are the astronomical irradiance, which rests on simple geometric analysis, atmospheric losses, reflection losses at the sea surface and the absorption in the water column.

3.1. Astronomical irradiance

The light irradiance (in W m^{-2}) above the atmosphere depends on astronomical conditions (date t, daytime τ, geographical latitude φ). For convenience τ is taken as angle between $-\pi$ and π with $\tau = 0$ at noon. In the same way $\vartheta(t)$ describes the time of the year as angle with $\vartheta = 0$ at June 21 (t is the time of the year expressed in days):

$$\vartheta(t) = 2\pi \frac{t - 172}{365}$$

With these definitions the astronomical irradiance is:

$$I_{ast}(t, \tau, \varphi) = I_{solar} \cdot \max(0, \cos\alpha)$$

where $I_{solar} = 1368$ W m^{-2} is the solar constant, and α is the angle between sun and the local normal vector depending on φ, ϑ and τ:

$$\cos\alpha = \sin\beta \sin\varphi + \cos\beta \cos\varphi \cos\tau$$

with $\sin\beta = \sin\rho \cdot \cos\vartheta$

The angle $\rho = 23.5°$ is the inclination of the pole axis. Sunset and sunrise $\pm\tau_s$ are defined by $\cos\alpha = 0$:

$$\tau_s = \arccos(-\tan\varphi \tan\beta)$$

The length of the light day as a fraction of the 24-hour day is then:

$$\ell = \frac{\tau_s}{\pi}$$

Of special interest are the noon and average irradiances:

$$\cos\alpha_{noon} = \sin\beta \sin\varphi + \cos\beta \cos\varphi$$

$$\overline{\cos\alpha} = \sin\beta \sin\varphi - \cos\beta \cos\varphi \frac{\sin\tau_s}{\tau_s}$$

3.2. Irradiance in the water column

The irradiance just below the water surface is the astronomical irradiance reduced by loss factors: cloud cover, absorption and reflection on the water surface. The cloud cover has the largest effect. Let cloud be the covered fraction of the sky averaged over the light day, then the subsurface irradiance is determined by the empirical functions A(cloud) and B(cloud) (Dobson and Smith, 1988):

$$I_s = \text{pafr} \cdot I_{ast} \cdot (A(\text{cloud}) \cdot \cos\alpha + B(\text{cloud}) \cdot \cos^2\alpha)$$

Here, additionally, account is taken of the fact that only a fraction of the light energy arriving at the sea surface can be used in photosynthesis, the so-called photosynthetically active fraction pafr.

The conceptional time step of the ERSEM model is the day. Hence, the light module delivers irradiance to the primary producer module as an average I_s over the daily light period (sunrise to sunset, without pafr) and the length of this period as fraction ℓ of the day. Both are functions of date t and latitude φ. The daily primary production has to be calculated as an integral over the day. Day–night or morning–evening differences are treated implicitly. Therefore an approximative reconstruction of the full daytime dependence of the irradiance including atmospheric losses and reflections is needed:

$$I_0(\tau) = I_s \cdot pafr \cdot \left(\cos(\tau/2\ell) + \cos^2(\tau/2\ell)\right) \cdot \frac{2\pi}{4+\pi}$$

This formula is similar to the approximation of Dobson and Smith (1988). A pure cosin would overestimate the irradiance in the morning and in the evening when absorption and reflection are higher. The factor $2\pi/(4+\pi)$ is the inverse of the integral over $\cos + \cos^2$, it makes $\bar{I}_0 = I_s \cdot pafr$.

For later use the noon (n) irradiance and the afternoon (a) irradiance (half-time between noon and sunset) are given:

$$I_0(\mathrm{n}) = \bar{I}_0 \cdot 1.7596$$

$$I_0(\mathrm{a}) = \bar{I}_0 \cdot 1.0620$$

Let now σ be the extinction coefficient in the water column. The photosynthetic active fraction of light is not uniform, its components are absorbed differently. Therefore the effective extinction coefficient is depth dependent, and larger close to the surface (Taylor and Joint, 1990). This aspect is neglected in the following, a constant σ is assumed and thus the photosynthetic active irradiance $I(z)$ decreases exponentially with depth z in the model:

$$I(z) = I_0 \cdot \mathrm{e}^{-\sigma z}$$

This will be the case in any layer, and is not confined to the surface layer. Then $z \in [0, D]$ is the depth in meters below the upper boundary of the considered layer of thickness D and I_0 is the irradiance at the upper boundary. The extinction constant σ is taken to be constant within the layers but may differ between layers. In a box model like ERSEM is now, the layers generally are thick ($D \approx 30$ m) but by specifying each D explicitly, the model can be used with an arbitrary number of layers.

3.3. Production in the water column

For the calculation of the daily average production *prod* (m^{-3}) the productivity p has to be integrated (averaged) over depth z and over day time τ ($I_0(\tau)$ is the day time dependent irradiance at the upper boundary of the considered layer):

$$prod = \frac{1}{2D} \int_{\mathrm{day}} \int_{\mathrm{layer}} p\left(I_0(\tau)\,\mathrm{e}^{-\sigma z}\right) \mathrm{d}z\,\mathrm{d}\tau$$

Two fundamental and questionable assumptions are hidden in this basic approach: primary productivity is in reality not additive in space and time. The production of a cell is assumed to be dependent only on the irradiance at its position in space and time and not on the light history of the cell. We know, however, that there are limiting dark reaction, light adaptation and irreversible damage. Further it is assumed that the phytoplankton density distribution is uniform over the considered (mixed) layer, which is not necessarily true. To get the production in mg C m^{-3} d^{-1}, the specific productivity p has to be multiplied with the density of the considered phytoplankton group. The vertical transport due to turbulence in the mixed layer is fast but not so fast that the phytoplankton density is constant over this layer because the characteristic reproduction times are comparable with mixing times. These problems are ignored.

First the integration over depth z is carried out. Let $p(I(z))$ be the productivity per m^3, then the average light-dependent productivity as a function of I_0 in the considered layer of thickness D is:

$$f(I_0) = \frac{1}{D} \int_0^D p\left(I_0 \cdot \mathrm{e}^{-\sigma z}\right) \mathrm{d}z$$

$$= \frac{1}{\sigma D} \int_{I_D}^{I_0} \frac{p(I)}{I}\,\mathrm{d}I$$

provided that the density and properties of the primary producer are homogeneous in the layer. In this formula $I_D = I_0 \cdot \mathrm{e}^{-\sigma D}$ is the irradiance at the lower

boundary of the layer. The second integration of $f(I_0)$ over the day time τ can be approximated with Simpson's rule:

$$prod = \frac{1}{\text{day}} \int_{\text{day}} f(I_0(\tau))\, \mathrm{d}r = \ell \cdot \overline{f(I_0)}$$

$$\cong \ell \cdot \frac{1}{6} (f(I_0(\mathrm{n})) + 4(I_0(\mathrm{a})))$$

The corresponding rectangle integration would simply lead to $prod = \ell \cdot f(\overline{I_0})$.

The rectangle approximation generally overestimates the production. It cannot take into account effects such as the effective shortening of daylength on very cloudy days and the suppression of production at noon on very light days due to the nonlinearity of the productivity function $f(\overline{I_0}) \neq \overline{f(I_0)}$.

The functional form of $p(I)$ cannot be precisely defined. The reason for the uncertainty is manifold. It is an empirical curve with three parameters, but $p(I)$ cannot truly be measured because the production is not proportional to the illumination time. The shapes of the p/I curves depend on the details of the experimental setup, not only on the parameters. Usually a functional form is selected, where the integration can easily be carried out. Eight different formulations have been considered in this model:

(a) $p(I) = p_0 \cdot x\mathrm{e}^{1-x}$

(b) $p(I) = p_0 \cdot \dfrac{2x}{1+x^2}$

(c) $p(I) = p_0 \cdot \dfrac{4x}{(1+x)^2}$

(d) $p(I) = p_0 \cdot \dfrac{(2+a)x}{1+ax+x^2},\ a \geq 0$

(e) $p(I) = p_0 \cdot \min\left(x, \max\left(\dfrac{a-x}{a-1}, 0\right)\right),\ a \geq 0$

(f) $p(I) = p_0 \cdot \min(1, x)$

(g) $p(I) = p_0 \cdot \dfrac{4x}{1+4x}$

(h) $p(I) = p_0 \cdot \dfrac{4x}{\sqrt{3+16x^2}}$

All these empirical forms have the 'scaling' property: p is dependent on $x = I/I_{\text{opt}}$ only, where I_{opt} is the variable describing the irradiance necessary for optimal productivity. Steele's function (Steele, 1962) (a) in this list of p/I algorithms is one of the most frequently used. The hyperbolic curves (b) and (c) are special cases of (d) ($a = 0$ and 2, Klepper et al., 1988). They are introduced to study the effect of more or less light inhibition. The function (e) is a piecewise linear curve and (f) is a simple ramp. In all cases (a) to (f) for $x = 1$ the productivity p assumes the maximal value p_0. The ramp (f) and the remaining forms (g) and (h) show no light inhibition. Form (g) represents the Monod function. The last (h), is known as Smith's equation (Jassby and Platt, 1976). It is half way between a scaled ramp $p(I) = p_0 \cdot \min(1, 2x)$ and Monod. These forms also have the 'scaling' property. However, no optimal irradiance exists. For compatibility with the other relations we define for these cases:

$$I_{\text{opt}} = 4I_{\text{half}}$$

where I_{half} is the irradiance with half maximal productivity. Hence, for $x = 1/4$ the production is $p_0/2$. Many other p/I relations have been invented and used (Kirk, 1983). It can hardly be said that one is 'the best', because the experimental results vary strongly. For the further calculation it is convenient to work with a dimensionless function $q(x)$ with:

$$p(I) = p_0 \cdot x \cdot q(x)$$

The behaviour of the p/I function at low light is determined by the slope of p at $I = 0$:

$$\alpha = \left.\frac{\mathrm{d}p}{\mathrm{d}I}\right|_{I=0} = p_0 \frac{q(0)}{I_{\text{opt}}}$$

The slope α differs for the different functional forms:

$$\alpha = \frac{p_0}{I_{\text{opt}}} \left(\mathrm{e}, 2, 4, 2+a, 1, 1, 4, 4/\sqrt{3}\right)$$

where the numbers in the brackets correspond to the cases (a) to (h). This is important, because if one wants to investigate the effect of the light inhibition one should compare functions with the same α! This can be done conveniently by using the same formulas with x substituted by a scaled variable:

$$x \to x \frac{\alpha\ (\text{wanted})}{\alpha\ (\text{as it is})}$$

The parameters p_0 and I_{opt} must not be changed. The slope α for the last case shows that a definition $I_{\text{opt}} = 4I_{\text{half}}$ makes Smith's equation (h) comparable with Steele's form (a).

With the help of the function $q(x)$ the depth integral can be expressed as:

$$f(I_0) = \frac{p_0}{\sigma D} \int_{x_D}^{x_0} q(x)\,dx$$

$$\text{with } x_0 = \frac{I_0}{I_{opt}},\ x_D = \frac{I_D}{I_{opt}}$$

The integral is a dimensionless figure which cannot exceed e in case (a) and π in case (b) and it can be carried out analytically in all cases ((d), (e) not given):

(a) $q(x) = e^{1-x}$ $\quad \int q(x)\,dx = -e^{1-x}$

(b) $q(x) = \frac{2}{1+x^2}$ $\quad \int q(x)\,dx = 2\arctan(x)$

(c) $q(x) = \frac{4}{(1+x)^2}$ $\quad \int q(x)\,dx = \frac{-4}{1+x}$

(f) $q(x) = \min\left(\frac{1}{x}, 1\right)$ $\quad \int q(x)\,dx = \begin{cases} x & x < 1 \\ 1 + \ln x & x > 1 \end{cases}$

(g) $q(x) = \frac{4}{1+4x}$ $\quad \int q(x)\,dx = \ln(1+4x)$

(h) $q(x) = \frac{4}{\sqrt{3+16x^2}}$

$$\int q(x)\,dx = \ln\left(4x + \sqrt{3+16x^2}\right)$$

For thick layers as in the standard ERSEM version the daily production integral is limited in the cases (a) and (b) to approximately:

$$prod \cong \ell \cdot f(I_0) \cong p_0 \frac{3\ell}{\sigma D}$$

More important, this upper estimate is a good absolute approximation if $3/\sigma \leq D$ and the irradiance I_0 at the layer surface substantially exceeds I_{opt}. In the upper ERSEM boxes these conditions are fulfilled from February to November. In the cases without light inhibition the situation is slightly different. But also in these cases there is only a weak dependence on the surface irradiance I_0. A tenfold increase of I_0 leads only to an increase of a factor $\ln 10 \cong 2.3$ in the production. The total irradiance-forced primary productivity depends on the factors:

- light fraction of the day, ℓ
- extinction σ
- surface irradiance I_0 (weakly)
- the group and nutrient dependent maximal productivity p_0.

The first three factors are combined in a dimensionless light limitation factor:

$$e_I = \frac{prod}{p_0}$$

$$\cong \frac{\ell}{\sigma D} \frac{1}{6} \left[\int_{x_d(n)}^{x_o(n)} q(x)\,dx + 4 \int_{x_1(a)}^{x_0(a)} q(x)\,dx \right]$$

$$\approx \frac{\ell}{\sigma D} \int_{x_D}^{x_0} q(x)\,dx$$

with for surface boxes the noon values $x_0(n) = I_0(n)/I_{opt}$ and $x_D(n) = x_0(n) \cdot e^{-\sigma D}$, and similar for the afternoon $x_0(a)$ and $x_D(a)$. For deeper layers $I_0(n)$ [and $I_0(a)$] the irradiance arriving at the upper boundary of these layers is: $I_0(n)$ (lower box) $= I_0(n) \cdot e^{-\sigma D}$. Note that σ may be different in upper and lower boxes.

The factor e_I can be interpreted as the fraction of the total daily space–time volume $D \cdot$ day in which primary production takes place. Assuming Steele's function (a), the approximate form is very illuminating:

$$e_I \cong \frac{3\ell}{\sigma D}$$

The turbidity in the North Sea is such that the irradiance declines to e^{-1} in 3–5 m ($\sigma = 0.2 \ldots 0.3$ m^{-1}). In coastal areas the extinction coefficients are generally much higher. Due to the fact that p has a maximum which is quite narrow in Steele's function the productivity is high only in a limited fraction of the water column. The thickness of the productive layer can be estimated to be about $3/\sigma$. The productivity is nearly *independent* of the surface irradiance because with varying I_0 only the position of the productive layer shifts up and down, but its thickness does not change. For a given depth D only daylength and extinction σ matter, and, of course, the maximal rate p_0 which is temperature and nutrient dependent. Somehow this result seems unsatisfactory. It has, indeed, limits: when the productive layer extends to the bottom where D is small (f.e. in shallow coastal areas), or if the layer intersects the surface (in winter). But, if light–shade adaptation exists, the adaptation of I_{opt} to the prevailing light conditions will keep this

layer within the mixed layer [0, D]. With $\sigma = 0.25$ m^{-1}, $D = 30$ m and $\ell = 0.5$ (12 h light period) one has $e_I \approx 0.2$ as an orientation value.

As mentioned above, this consideration changes, but only slightly, if p/I curves without light inhibition are analysed. Here the surface irradiance has a certain effect, because the thickness of the productive layer increases logarithmically (very slowly) with I_0. This dependence is, however, further reduced by light adaptation of the scaling parameter I_{opt} (Section 3.4).

3.4. Light adaptation

In the model, it is assumed that the parameter I_{opt} (optimal light) in the p/I function is not a fixed parameter but a variable. Algae can adapt to widely varying light conditions. Cells circulate in the mixed layer by turbulence and their individual I_{opt} reflects their recent light history. The adaptation occurs typically in only a few days. This is short enough to assume the same light adaptation for all algae in a well mixed layer, and it is long enough to assume adaptation to seasonal changes but not to weather conditions. The adaptation is limited:

$$I_{opt}^{min} \leq I_{opt} \leq I_{opt}^{max}$$

In principle, these limits can be assumed to be different for the four functional groups. In the model it is assumed that the adaptation occurs to the daily average light at certain depth D_a (adaptation depth) below the surface. The adaptation itself is described by a simple relaxation process with time constant r_I. The parameter I_{opt} shifts toward a changing 'equilibrium' value $\tilde{I}_{opt}$:

$$\tilde{I}_{opt} = \min\left(I_{opt}^{max}, \max\left(I_{opt}^{min}, \overline{I(D_a)}\right)\right)$$

$$\frac{d}{dt} I_{opt} = r_I \cdot \left(\tilde{I}_{opt} - I_{opt}\right)$$

The average of $I(D_a)$ is taken over the light day:

$$\overline{I(D_a)} = I_0 \cdot e^{-\sigma D_a}$$

The phytoplankton property I_{opt} has to be transported like a substance and therefore it has to be bound to biomass in order to account for the vertical exchange of phytoplankton with a different light history and consequently different I_{opt} properties. It is transported in the form of the product $\left(\sum P_c\right) I_{opt}$. All groups of primary producers have to be taken into account.

In the case of light inhibition a real optimal irradiance exists. Then the solution of the equation:

$$\frac{d}{dI_{opt}} prod\Big|_{\tilde{I}_{opt}} = 0$$

expresses an optimisation principle which would be a good theoretical base for a practical formulation of the adaptation. It leads to an $\tilde{I}_{opt}$ which optimises the production in the considered layer [0, D]. It is a natural assumption that phytoplankton changes its I_{opt} in the direction of this optimum, as long as the physiological limit I_{opt}^{min} allows this. In the case of a scaling productivity, the optimal I_{opt} is reached when the productivities at the upper and lower border of the considered layer are equal. This contradicts the observations which suggest that productivity has its maximum close to the surface (P. Ruardij, pers. comm.). Obviously a short time close to the surface enables the cells enough production and causes adaptation to higher intensities. Either the assumption that light adaptation leads to optimal production is wrong, or a scaling p/I curve is not realistic, or hidden loss terms in the case of low I_{opt} are important (higher activity respiration or danger of damage). Such effects and more realistic I_{opt} values could easily be implemented by sacrificing the scaling property but keeping the optimisation principle. However, model experiments did not show a very large influence of the exact way of modelling the light adaptation on the results. Important is only that there is *some sort* of adaptation. It keeps the dependence on the absolute (surface) irradiance low in summer. In winter the light limitation is important due to $\tilde{I}_{opt} < I_{opt}^{min}$. Otherwise the simulations would not reproduce the low winter phytoplankton concentrations.

4. Results and sensitivity analysis

4.1. The reference run

The set of standard parameters for the phytoplankton groups is given in Table 1. The simulation results of the ERSEM 15-box version obtained with this set of parameters and with the Oldenburg ben-

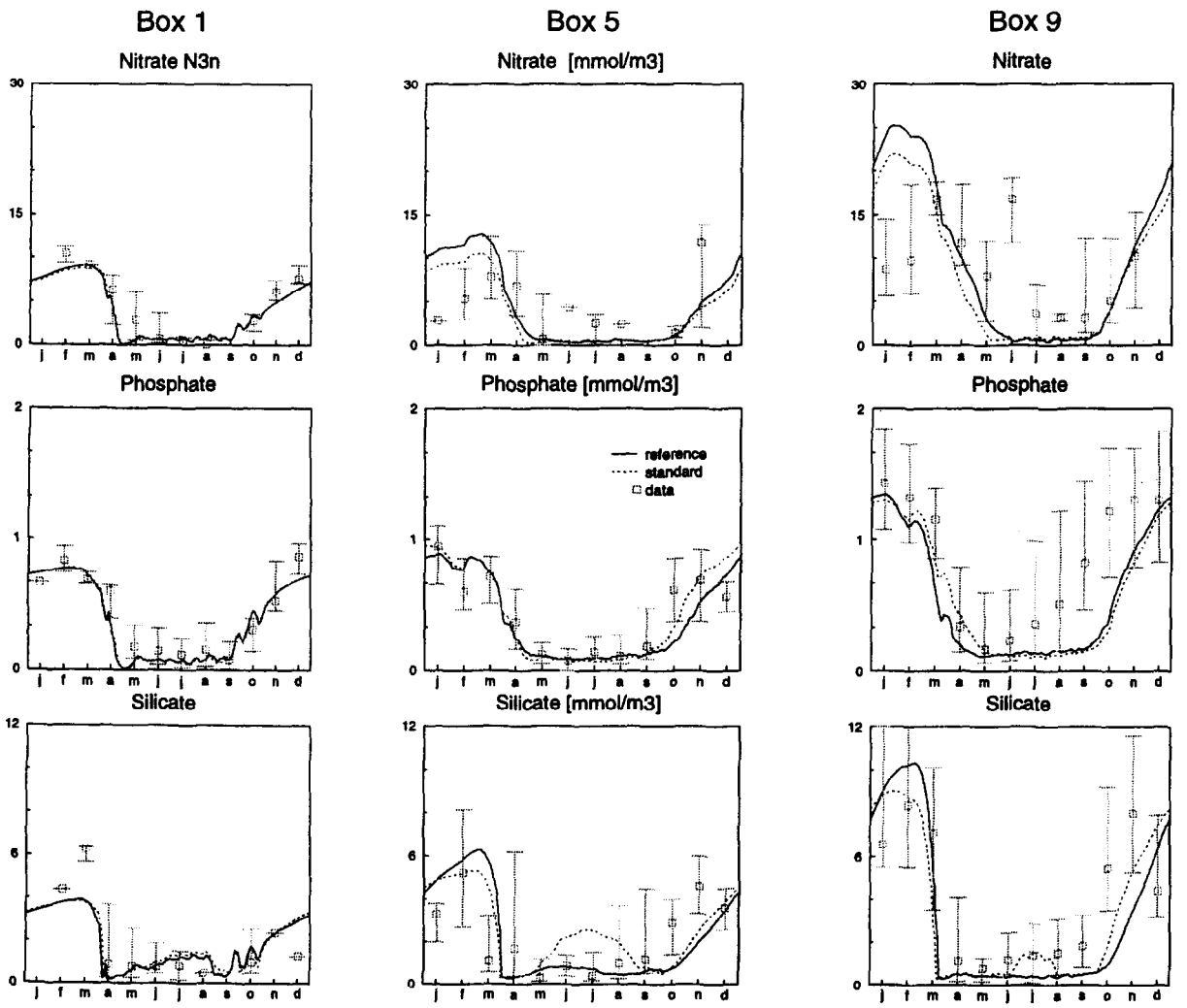

Fig. 1. The simulated concentrations of nitrate, phosphate and silicate in mmol m^{-3} for the boxes 1, 5 and 9. Results of the reference run with the Oldenburg nutrient module and of the standard run with the NIOZ nutrient module are given together with measurements.

thic nutrient module are presented in Figs. 1–3. In these figures also the results of the standard ERSEM run, obtained with the NIOZ benthic nutrient module, and calibration data are given. Both versions of ERSEM contain the identical phytoplankton module, using the ramp formulation as p/I algorithm.

In the sensitivity runs the Oldenburg benthic nutrient module has been used as reference, since the differences with the standard benthic nutrient module are slight (see Figs. 1–3) and the Oldenburg module, being more implicit, is computationally much less expensive.

The curves in Figs. 1–3 represent approximately an equilibrium cycle, which was achieved by a simulation run over ten years with perpetual-year forcing. The transport forcing for the year 1989 was used (Lenhart et al., 1995). The observations indicated in Figs. 1–3 are taken from the validation data used in ERSEM. The nutrient, phytoplankton and chlorophyll data are derived from the NERC North Sea data base (BODC) and the ECOMOD data base, compiled by the Institut für Meereskunde in Hamburg (Radach and Pätsch, 1997.

The spatial structure of the 15-box version is

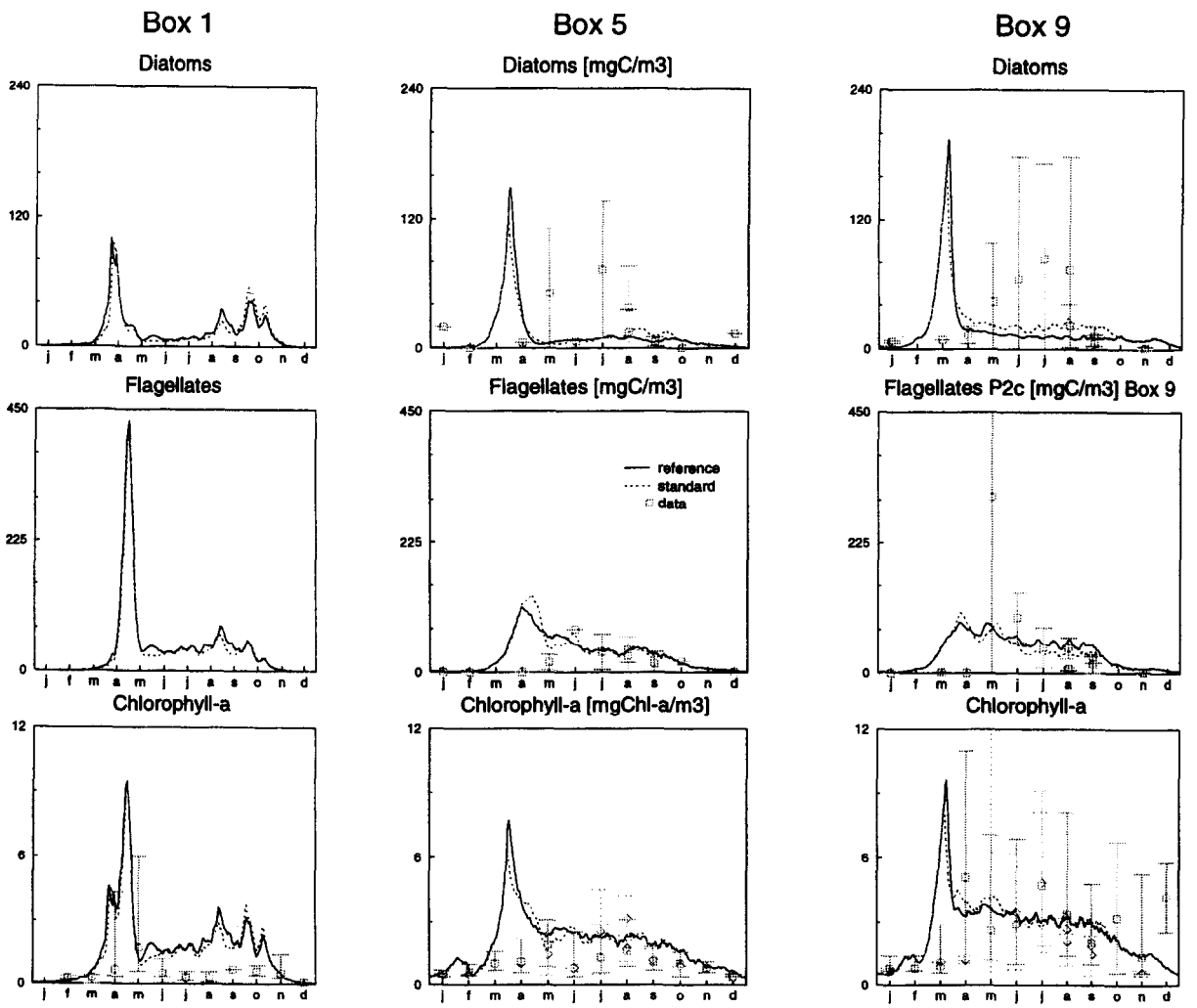

Fig. 2. The simulated concentrations of diatoms, flagellates (in mg C m^{-3}) and chlorophyll (in mg Chl-*a* m^{-3}). See Fig. 1.

described in ERSEM I (Baretta et al., 1995). The results of three boxes are shown: box 1, the northern North Sea; box 5, central North Sea; and box 9, the German Bight.

Although it is clear that the primary production module does not operate in isolation and that the model results are the end product of many interacting processes, there are a few system aspects, where the formulation of primary production processes and their interaction with the physical forcing define almost single-handedly how the system behaves. As only the phytoplankton groups transform dissolved inorganic nutrients into organic and particulate forms, the spring decline in the dissolved nutrients is caused by the phytoplankton. The onset and rate of this decline, as well as the recovery in autumn to winter concentrations are strongly different in the different regions of the North Sea (Fig. 1), but also the regional differences are captured quite well by the model. The model results predict a diatom spring bloom, in all boxes followed by a flagellate bloom (Fig. 2). The (scarce) data, resolved to functional groups, do not show a spring bloom at all, but suggest the occurrence of intermittent summer blooms. The flagellate phytoplankton standing stock is reproduced reasonably well for the summer period

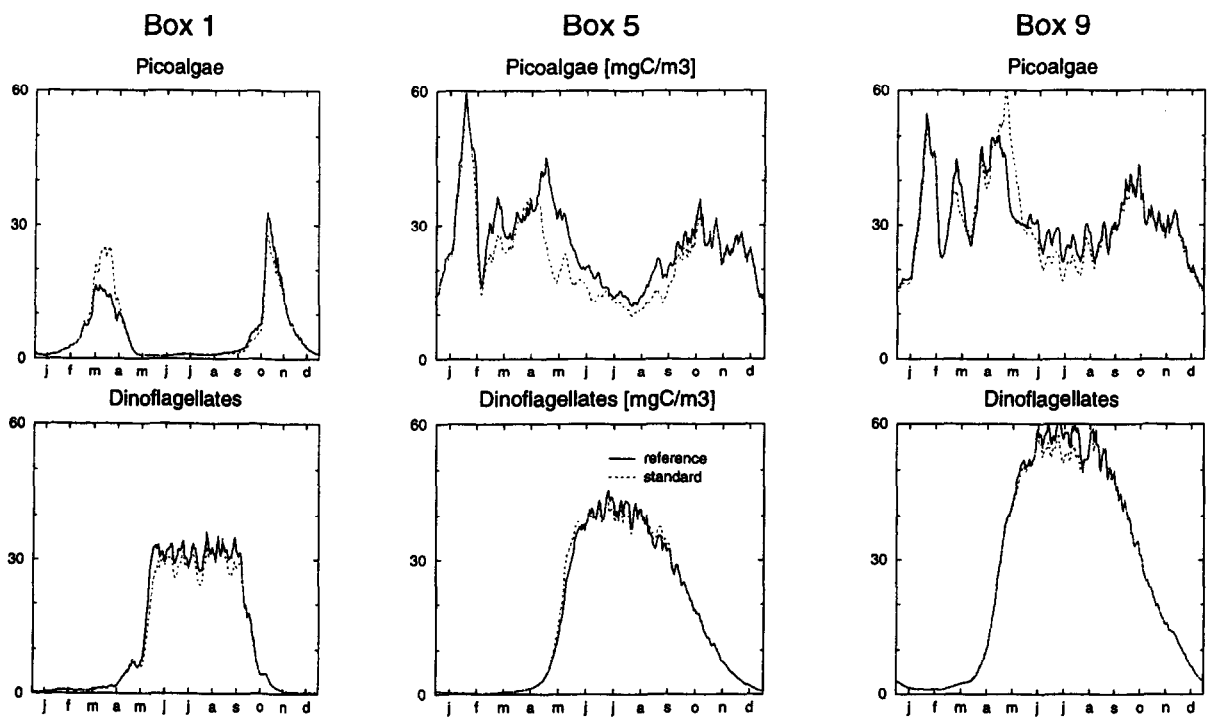

Fig. 3. The simulated concentrations of picoalgae and dinoflagellates (in mg C m^{-3}). See Fig. 1.

in the central North Sea and the German Bight, but the diatom biomass is underestimated. The standing stock of picoalgae tops out at around 50 mg C m^{-3}, with a small end-of-winter bloom, which is halted by heterotrophic nanoflagellate grazing.

Total phytoplankton biomass, as represented by the uncertain proxy of chlorophyll-*a*, is overestimated in the north in summer, and in the other regions during spring. The winter concentrations are reproduced very well everywhere, as are the summer values in the central and southern North Sea.

Table 1
Relevant parameters as used in the ERSEM-II primary production module

Name	Unit	Meaning	Values
r_{ass}	d^{-1}	maximal production rate	2.5, 2.7, 4.0, 1.5
r_{bas}	d^{-1}	basal respiration	0.16, 0.10
q_{ex}	–	exudation under nutrient stress	0.05, 0.20, 0.20, 0.05
q_{res}	–	respired fraction of production	0.10, 0.25
pafr	–	photosynthetic active fraction	0.5
D_a	m	adaption depth	10
I_{opt}^{min}	W m^{-2}	minimum for optimal light	4
I_{opt}^{max}	W m^{-2}	maximum for optimal light	80
r_I	d^{-1}	light adaption rate	0.25
Q_{10}	–	Q_{10}-value	2.0

A row of four given values corresponds to the four functional groups of primary producers: diatoms, autotrophic flagellates, picoalgae and dinoflagellates; two values to diatoms and others; one value is valid for all groups. For the full parameter list see Baretta-Bekker et al. (1997).

4.2. The generation time

The parameters with the highest sensitivity are the gross production rate r^{ass} and the basal respiration rate r^{bas}. Together with the loss factors activity respiration q^{res} and (minimal) exudation q^{ex} they determine the generation time T_2 (as potential doubling time) in the absence of nutrient limitations.

The doubling time T_2 can be calculated from the production rate r by:

$$T_2 = \frac{\ln 2}{r}$$

However, not the gross rate r^{ass} must be taken, but the maximal realised rate:

$$r = r^{ass} \cdot e_I \cdot (1 - q^{ex}) \cdot (1 - q^{res}) - r^{bas}$$

This formula follows from the model equations which are given elsewhere (Baretta-Bekker et al., 1997). The parameters q^{ex} and q^{res} give exudated and respired fractions and r^{bas} is the basal respiration rate. Nutrient limitations are absent and the temperature factor is also taken to be 1 (10°C). In Table 2 the reduction of the gross rates by respiration/exudation and by vertical spatial averaging to realised rates and

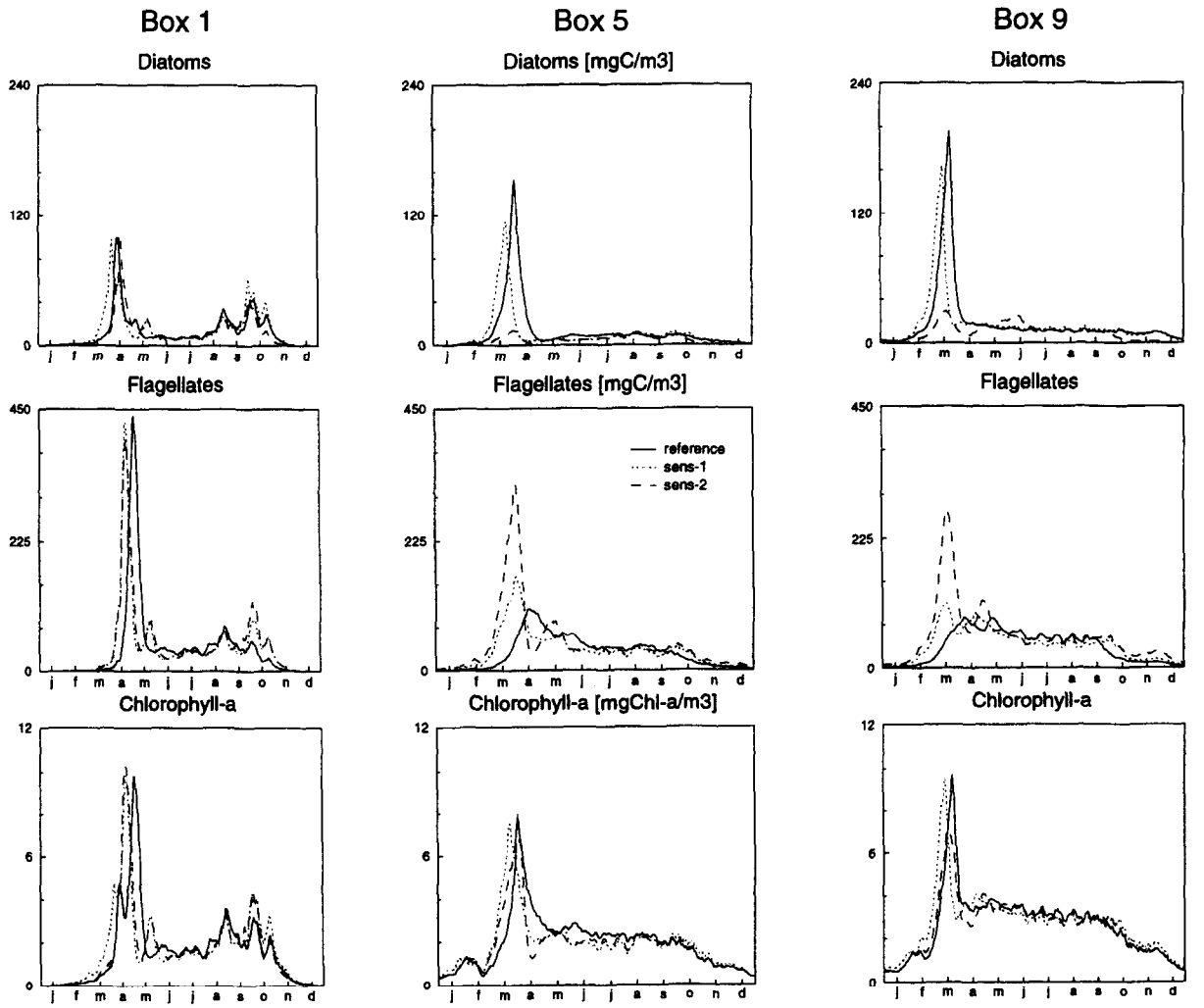

Fig. 4. The simulated concentrations of diatoms, flagellates (in mg C m^{-3}) and chlorophyll (in mg Chl-*a* m^{-3}) for sens-1, with all phytoplankton specific assimilation and rest respiration rates increased by 30% and for sens-2, where only the flagellates rates have been increased by 30% in comparison with the reference run.

Table 2
Realised primary production rates (r in d^{-1}) and doubling times T_2 (in d) under different light conditions

		r_{ass}	$r(e_I = 1)$	$r(e_I = 0.2)$	$r(e_I = 0.05)$	$T_2(e_I = 0.2)$
P1	Diatoms	2.5	1.99	0.28	−0.04	2.5
P2	Flagellates	2.7	1.52	0.22	−0.07	3.1
P3	Picoalgae	4.0	2.30	0.38	+0.02	1.8
P4	Dinoflagel.	1.5	0.97	0.11	−0.05	6.3

doubling times have been given.

The maximal realised rate under these conditions is $r(e_I = 1)$, then only respiration and minimal exudation losses are assumed. The maximal rate in the vertically averaged water column ($D = 30$ m, $\sigma = 0.25\ m^{-1}$) is $r(e_I \approx 0.2)$, here the values are taken as discussed in Section 3.3. It corresponds to a spring situation (12 h light, no nutrient limitation,

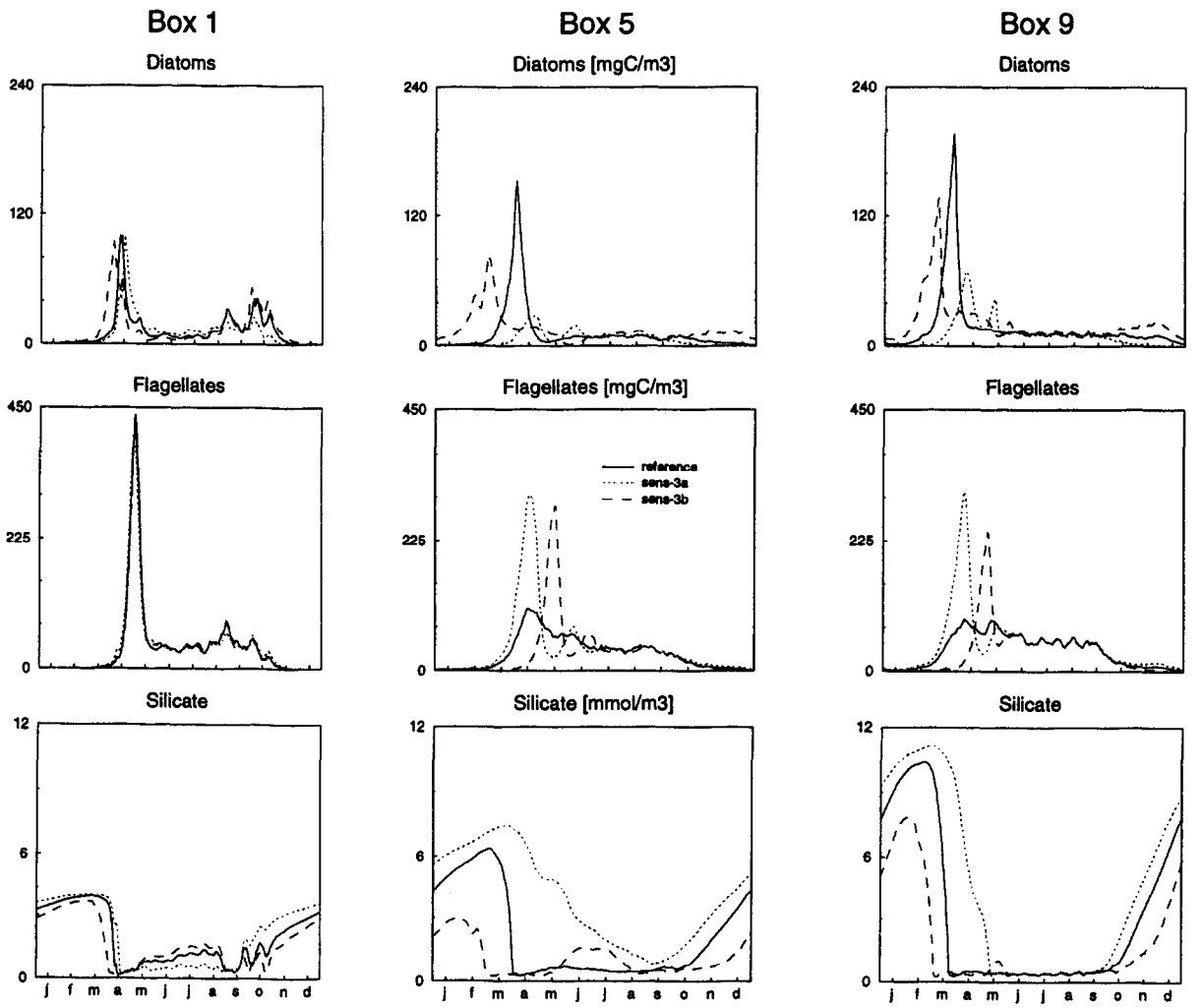

Fig. 5. The simulated concentrations of diatoms, flagellates (in mg C m^{-3}) and silicate (in mmol m^{-3}), with the specific rest respiration rate of diatoms increased (sens-3a) and decreased (sens-3b).

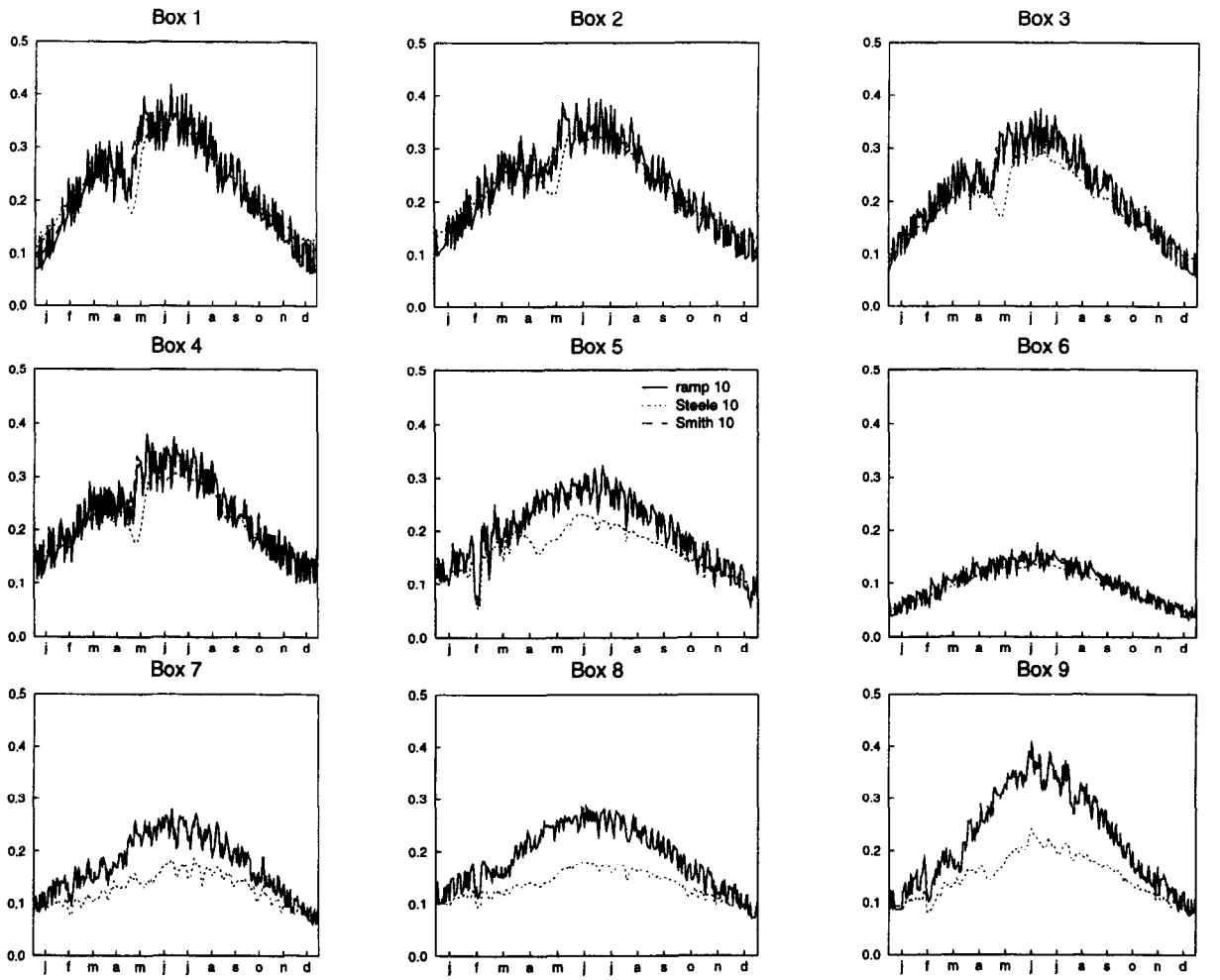

Fig. 6. Daily values of e_I as simulated with the three different p/I curves.

the temperature factor taken as 1). In summer N- and P-limitation can reduce the rates by another factor of 3 to 5, and diatoms are additionally subject to Si-limitation. The rate $r(e_I = 0.05)$ corresponds to a winter situation, where dark respiration r^{bas} can lead to negative net rates r. The doubling times in spring — vertically averaged over the upper mixed layer — are according to this estimate between 1.8 and 6 days. The spring bloom is mainly a diatom bloom in the model. This is due to the short doubling time of 2.5 d. Picoalgae with a still smaller doubling time grows even in winter in the model, hence it keeps its predators (mainly heterotrophic flagellates) active and therefore cannot escape in a pronounced spring bloom (Figs. 2 and 3).

4.3. Sensitivity analysis

The consequences to system function of decoupling the carbon assimilation and nutrient uptake dynamics will be discussed in Baretta-Bekker et al. (1997). As part of the sensitivity analysis the following simulations with modified parameters sets are carried out:

(1) sens-1: all r^{ass} and r^{bas} increased by 30%;
(2) sens-2: r^{ass} and r^{bas} only of flagellates increased by 30%;
(3) sens-3: r^{bas} of diatoms (a) increased and (b) reduced by 30%.

In all cases a three year simulation was carried out with initial values from the reference run. Then

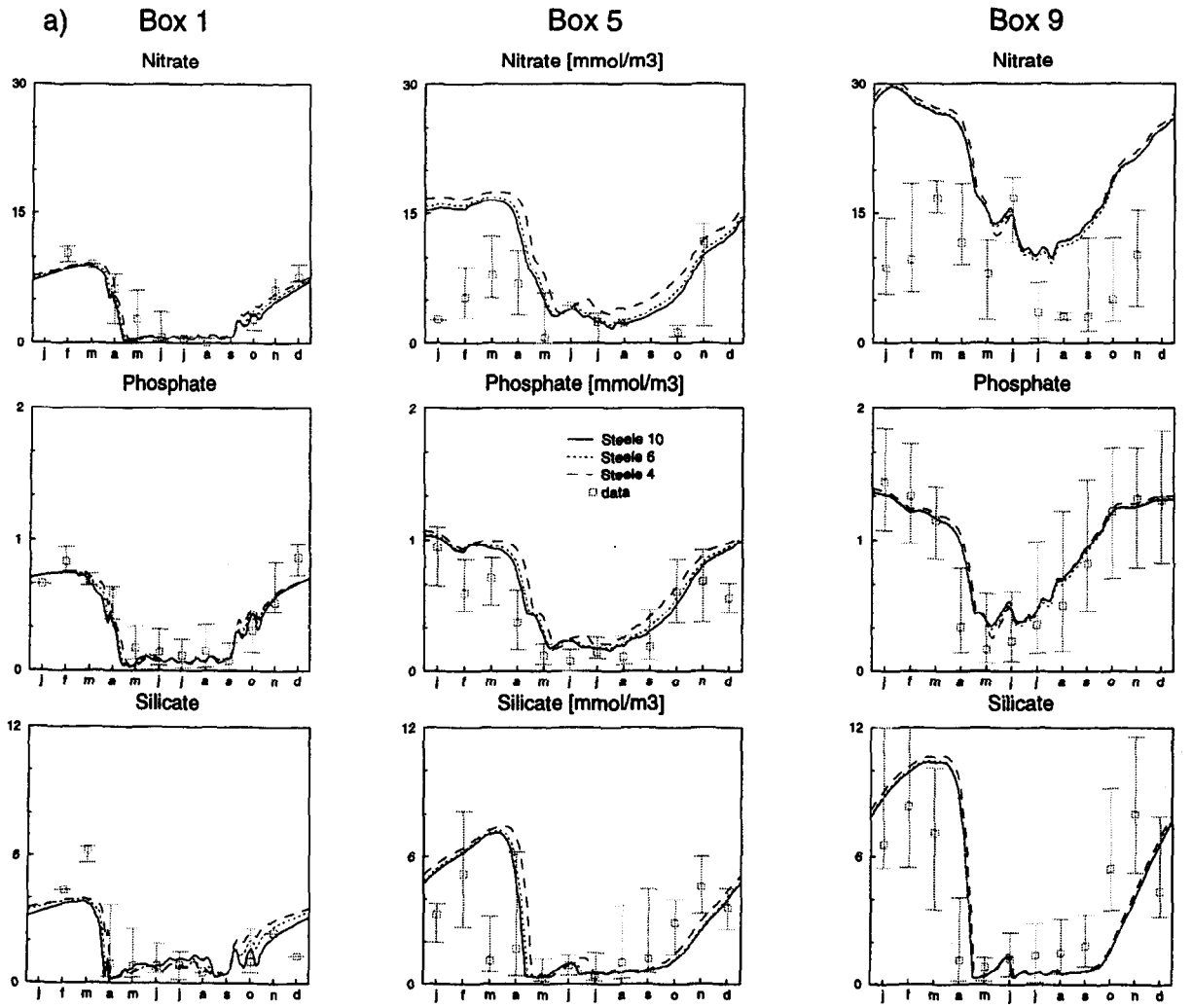

Fig. 7. The simulated concentrations of (a) nitrate, phosphate and silicate (in mmol m^{-3}) and (b) diatoms, flagellates (in mg C m^{-3}) and chlorophyll (in mg Chl-*a* m^{-3}) with three different adaptation depths (10, 6 and 4 m), with the p/I curve according to Steele (1974).

a new equilibrium cycle is nearly reached. The third year is shown. In case sens-1 (Fig. 4, dotted line) can be observed that due to the action of the several limitation factors the results are changed only moderately. In case sens-2 (Fig. 4, dashed line) the relative shift of flagellates against diatoms is obvious. Even the order of the spring peaks may change from diatom first to flagellates first. There is a slight increase in summer chlorophyll and a stronger depletion of nitrate. The case sens-3 (Fig. 5) is of special interest. Here growth rate and dark respiration are not changed by the same factor as in the cases sens-1 and sens-2. In this case the spring peak of the modified diatom is shifted in time or even does not occur at all. This is due to the fact that with reduced or increased light independent losses the net growth rate r is negative for a shorter or longer interval in winter. If r stays positive all winter, higher diatom concentrations in winter are produced by the model. Such high winter concentrations suppress the spring peak because of two reasons:

(1) grazers are already active at the beginning of the spring bloom because they have sufficient food in winter to maintain the standing stock,
(2) the nutrients have lower concentrations when the bloom starts and hence are depleted sooner.

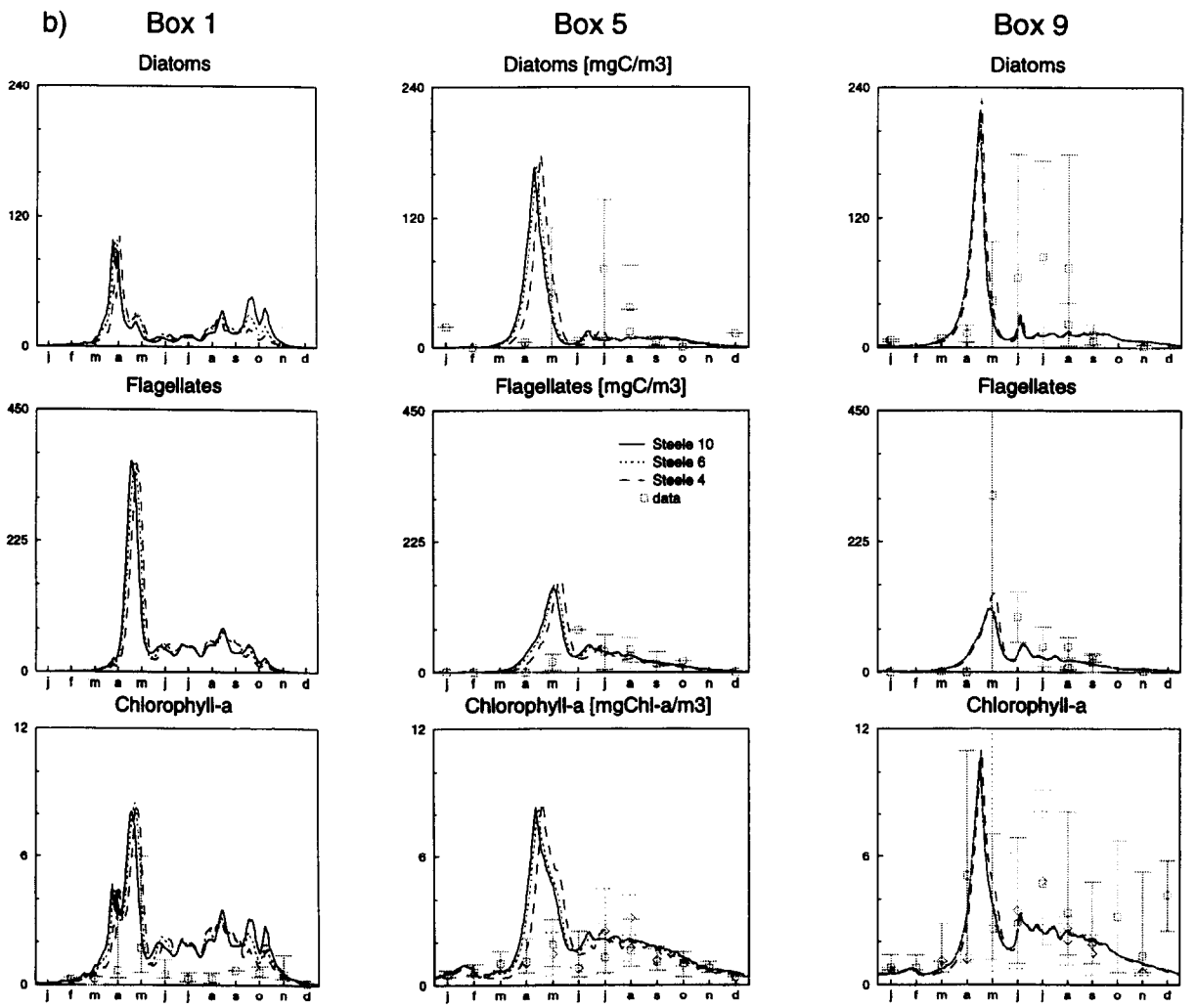

Fig. 7 (continued).

The other part of the sensitivity analysis is focused on the light forcing used in the model. Several types of light forcing have been implemented in the model and may be chosen by setting the appropriate switch value. Additionally, the depth where the phytoplankton adapts to the irradiance can be modified as well. A number of sensitivity analyses have been done of the effect of using different light forcings in combination with different adaptation depths on total primary production and nutrient cycling. The following three p/I curves are illustrated: Steele's formulation (a), ramp (f) and Smith's equation (h).

The ramp and Smith functions lead to lower production for low light ($\alpha = 1$ compared to $\alpha = e$ in Steele's formulation). It should be noted that the parameter I_{opt} has slightly different meanings in the three cases (see Section 3.3).

Comparing the three light forcing functions as they are expressed in the light limitation factor e_I we find that both the ramp formulation and the Smith formulation predict the light limitation to be much less (e.g., e_I has a higher value) in the turbid coastal boxes than the Steele formulation does. In the clear northern boxes the both formulations predict the light limitation to be stronger than Steele's formulation, resulting in lower primary production. Compared to Steele's formulation in the ramp and the Smith formulation the increased production above

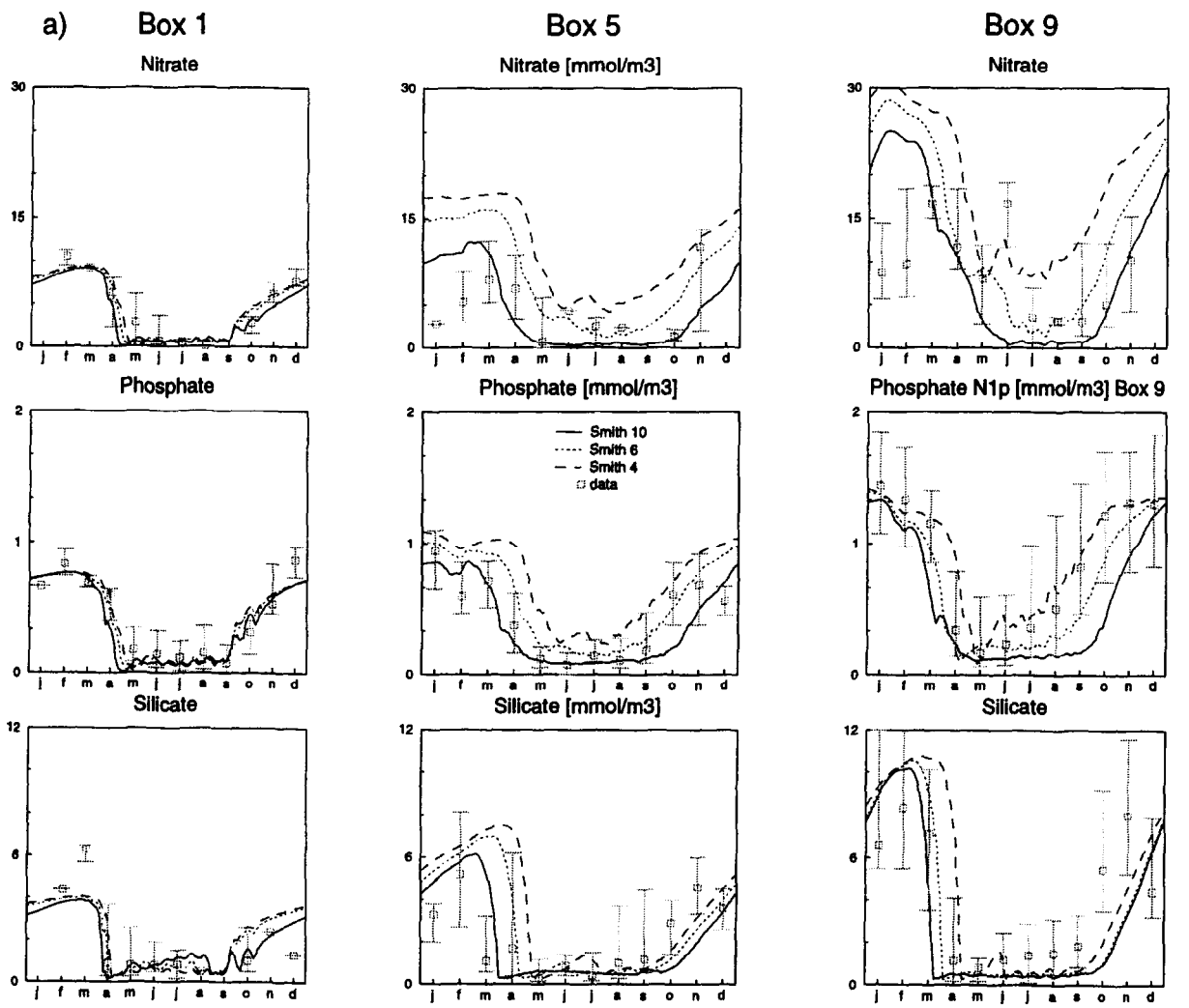

Fig. 8. The simulated concentrations of (a) nitrate, phosphate and silicate (in mmol m^{-3}) and (b) diatoms, flagellates (in mg C m^{-3}) and chlorophyll (in mg Chl-*a* m^{-3}) with three different adaptation depths (10, 6 and 4 m) with the Smith p/I formulation.

the adaptation depth is partly compensated by lower production at larger depths. The daily values of e_I, as calculated with the three different p/I curves are given in Fig. 6.

As the ramp and Smith functions give nearly identical results for all regions (Fig. 6) only results using Smith's formulation are shown in the following sensitivity analysis.

Changing the adaptation depth in three steps from 4 to 10 m for the different types of light forcing gave the following results. Adaptation depth has almost no influence on the results in Steele's formulation, neither in terms of timing of the spring bloom nor in terms of the production (Fig. 7). The other formulations are sensitive to the setting of the adaptation depth in that the spring peak is strongly shifted to later in the year when the adaptation depth is set to lower values (Fig. 8).

As the surface box is considered to be fully mixed, setting the adaptation depth to $\frac{1}{3}$ of the full depth seems a reasonable approximation. This is confirmed by the fact that the timing of the spring decline in dissolved inorganic nutrient concentration is reproduced best when using the Smith formulation with this adaptation depth (Fig. 8).

A reduced adaptation depth generally makes phy-

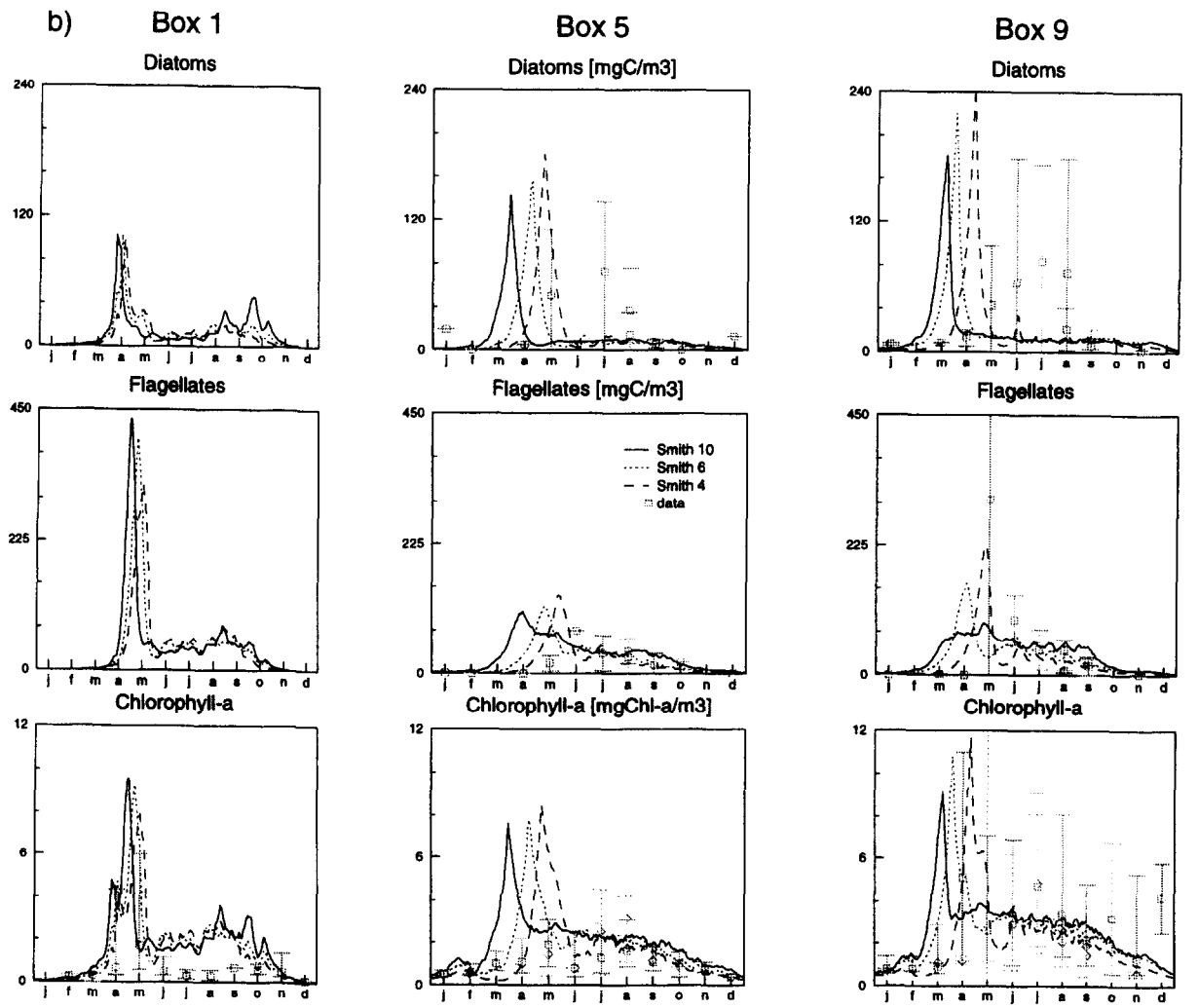

Fig. 8 (continued).

toplankton light adapted to higher irradiance levels, and hence less growth is possible at greater depths. The depth-integrated production is reduced, and the spring peak occurs later. In the Steele formulation, the adaptation depth does not make a significant difference (Fig. 7), but in the p/I formulations with less or no photoinhibition, it makes a large difference (Fig. 8). The sensitivity analysis suggests from the timing of nutrient depletion that the phytoplankton adaptation depth of 10 m is appropriate for a vertical resolution of 30 m as used in the model for the surface boxes. The calculated net annual primary productions using the different types of forcing are given in Table 3.

Choosing Smith instead of Steele as p/I formulation leads to large shifts in the regional distribution of annual net production, with production in the turbid coastal boxes with high riverine nutrient loads more than doubling. The annual net production in the other boxes decreases. The reason for this is that the light limitation of depth-integrated production as expressed in the e_I variable is stronger in the northern boxes when using the Smith p/I formulation especially in winter. Logically, this shift from light-limited towards nutrient-limited phytoplankton growth also manifests itself in the lower dissolved inorganic nutrient concentrations in the turbid river-influenced boxes 8 and 9.

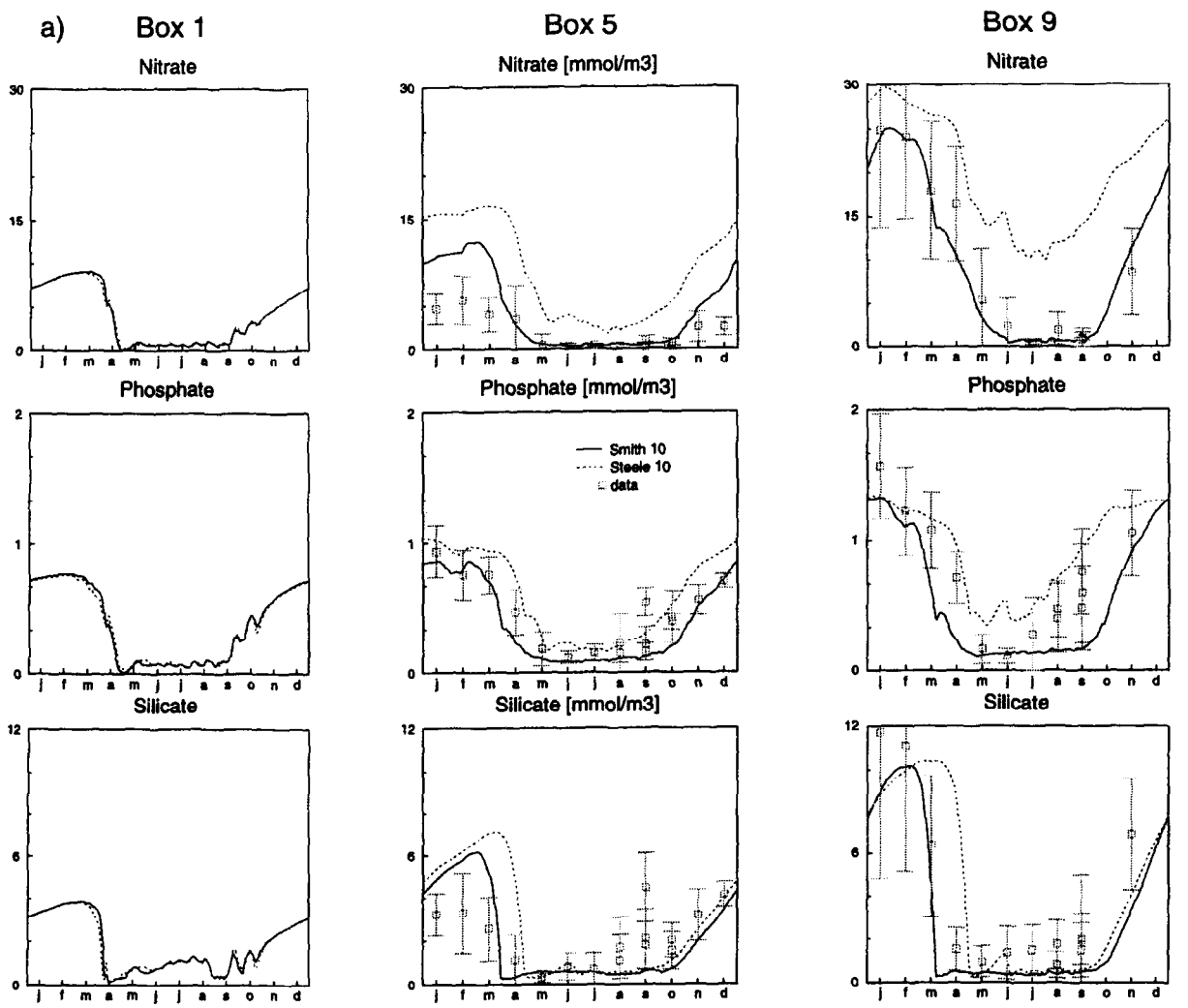

Fig. 9. The simulated concentrations of (a) nitrate, phosphate and silicate (in mmol m^{-3}) and (b) diatoms, flagellates (in mg C m^{-3}) and chlorophyll (in mg Chl-*a* m^{-3}) with two different light forcings. In all cases the adaptation depth is 10 m.

Table 3
Annual net primary production in g C m^{-2} a^{-1} for the two types of light forcing, with the adaptation depth set to 10 m

Box number	Steele	Smith	ERSEM I (Varela et al., 1995)	Joint and Pomroy (1993)
1	155	150	66	
2	151	149	189	
3	124	134	92	
4	167	159	204	
5	198	243	144	119[a] (box 4 and 5)
6	57	36	35	
7	89	187	123	79 (box 6 and 7)
8	128	321	148	199
9	139	392	190	
10	166	201	148	261 (box 9 and 10)

[a] Joint and Pomroy (1993) calculated average production for entire ICES regions, which cover the ERSEM boxes indicated.

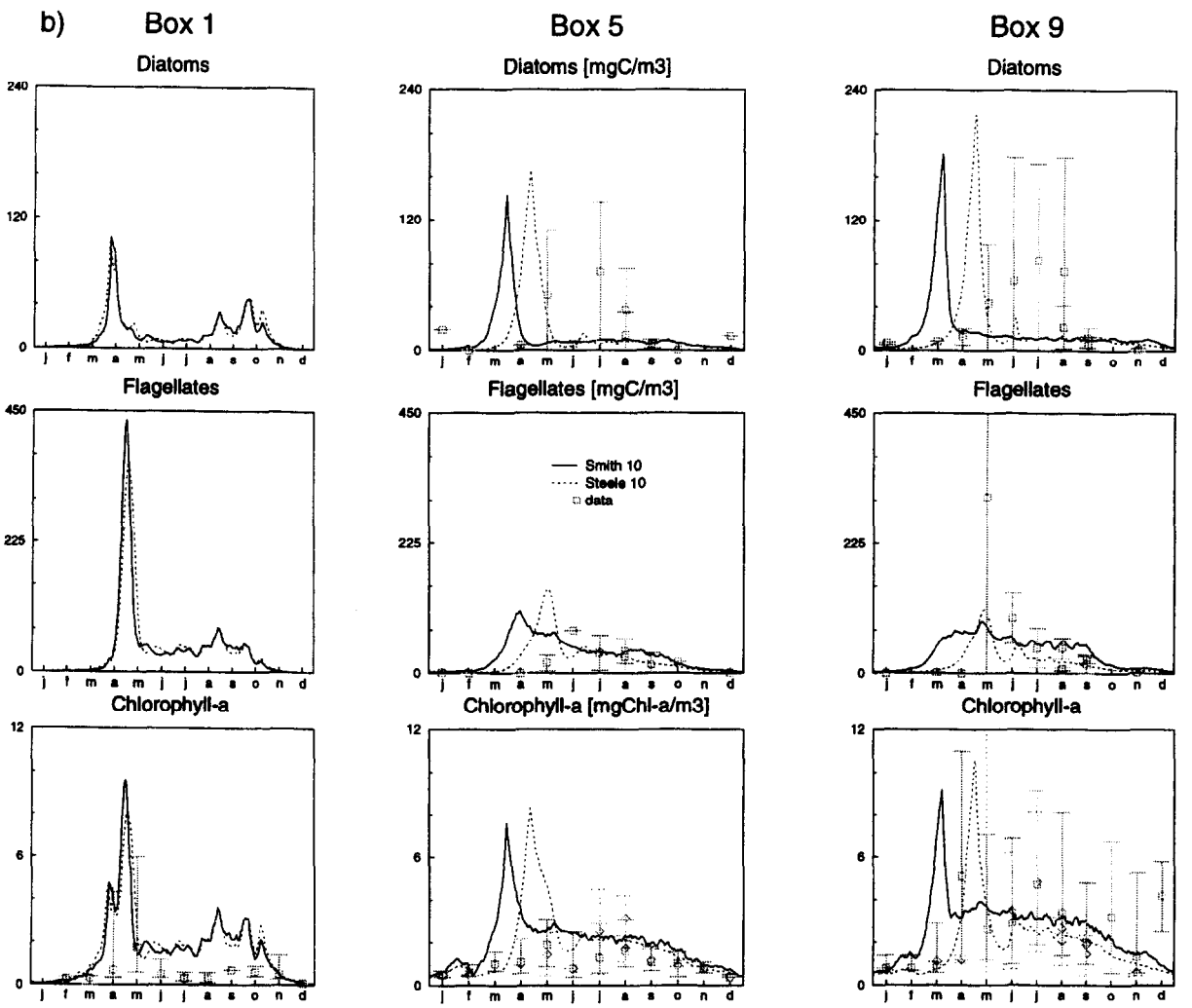

Fig. 9 (continued).

Due to the mentioned compensation in the Smith formulation compared to Steele the timing of the spring bloom is not affected at all in the northern boxes but is significantly earlier in the south (Fig. 9).

5. Discussion

The main requirement for the phytoplankton module in ERSEM is to properly describe the conversion of dissolved inorganic carbon and nutrients into particulate organic carbon. This objective is realised by the different phytoplankton groups that both control and are controlled by different combinations of environmental variables and, moreover, have different places in the food web due to size differences.

Of the abiotic environmental variables, light, temperature and nutrient availability play the major roles. The seasonality in the phytoplankton is completely controlled by the seasonality in the light, which may be modified by time varying suspended matter concentration in the water, which strongly determine the underwater light climate. Self shading only plays a minor role at the phytoplankton concentrations present, with the exception of the short spring bloom, when the light-limitation factor is clearly smaller in the northern boxes (Fig. 6).

From the sensitivity analysis using different for-

mulations for the p/I relationship it is clear that the model is very sensitive to this formulation, but mainly in those boxes which have a high turbidity, in other words the well-mixed coastal boxes in the Southern Bight. In the much clearer central and northern boxes the differences are much less. Only by forcing the primary producers with one of the p/I formulations that do not implicitly assume a strong photoinhibition in any type of water column, the model is able to attain the primary production levels in the turbid coastal areas that draw the dissolved inorganic nutrients down to the observed levels (Fig. 9), indicating that primary production and the concomitant transformation of dissolved inorganic nutrients into particulate and organic forms can be reproduced adequately by the model.

The most directly comparable primary production estimates for regions in the North Sea from literature are those given by Joint and Pomroy (1993) for the central and southern boxes. The model-calculated net primary production figures (Table 3) generally are considerably higher, as is to be expected, since Joint and Pomroy estimated primary production from observed chlorophyll-*a* concentrations, which necessarily underestimated total production as the chlorophyll-*a* removed by grazing and other loss processes cannot contribute to the production estimate.

Additionally, the regression between primary production as measured by ^{14}C incubations and observed chlorophyll-*a* concentrations is doubtful as Daneri (1992) has shown that bottle enclosure of seawater samples may lead to an underestimate by a factor two of carbon assimilation. Moreover, the net primary production estimates he gave for two tracked water bodies in box 8 in spring and autumn 1989 (the year used for the reference run) are 4.04 g C m^{-2} d^{-1} in April and 0.62 g C m^{-2} d^{-1} in October. The spring value far exceeds the model-calculated carbon assimilation, which is 1.65 g C m^{-2} d^{-1} in the corresponding period in April, but in October the model overpredicts the carbon assimilation rate at 1.59 g C m^{-2} d^{-1}. In both cases picoalgae have the largest contribution to the total carbon assimilation in the model, whereas in the field observations the high value in spring was due to a bloom of colony-forming flagellates and in autumn to a (developing) diatom bloom. This indicates the high local variability in system function, which cannot be captured by a coarsely resolved box model, but it also indicates that we still have a long way to go in properly representing biological interactions, and that the role of picoalgae in the system in autumn seems to be exaggerated in the model.

These discrepancies point out some of the problems in the model. The composition of the phytoplankton community in terms of the relative abundance and productivity of the component functional groups is as much determined by biotic interactions, mainly grazing interactions as by abiotic processes (light, nutrient availability). Even though the model may produce a reasonably correct figure for the total phytoplankton production, the relative contributions by the different phytoplankton groups are as strongly dependent on the food-web structure as on nutrient partitioning and -availability. The ERSEM model has a rigid food-web structure, which cannot account for the consequences of colonial forms not being grazed and thus escaping top-down control.

Comparing the primary production results from the new primary-production module with the results from ERSEM I (Varela et al., 1995), for the same spatial setup, we see that primary production in the new model is generally much higher, especially in the coastal boxes (Table 3), as Varela et al. (1995) have reasoned should be the case.

Acknowledgements

First and foremost, we gratefully acknowledge the support from MAST, under contract number MAS2-CT92-0032-C. We wish to thank the anonymous reviewers for their constructive comments, which helped us to improved the manuscript considerably. We thank Cora Kohlmeier and Frank Hamberg for the data-analysis and -display software tool MoVIE which allowed making sense of complex model results. Paul Turner is gratefully acknowledged for the availability of the graphical package XVGR, which made producing the figures for this paper almost enjoyable.

References

Anonymous, 1988. The ecosystem of the western Wadden Sea: field research and mathematical modelling. NIOZ-Rapport 1988-11.

Baretta, J.W., Ruardij, P., 1988. The ecosystem of a tidal flat estuary. Simulation and Analysis of the Ems Estuary. Ecological Studies 71, Springer, Berlin, 352 pp.

Baretta, J.W., Ebenhöh, W., Ruardij, P., 1995. The European Regional Seas Ecosystem Model, a complex marine ecosystem model. Neth. J. Sea Res. 33, 233–246.

Baretta-Bekker, J.G., Riemann, B., Baretta, J.W., Rasmussen, E.K., 1994. Testing the microbial loop concept by comparing mesocosm data with results from a dynamical simulation model. Mar. Ecol. Prog. Ser. 106, 187–198.

Baretta-Bekker, J.G., Baretta, J.W., Rasmussen, E.K., 1995. The microbial food web in the European Regional Seas Ecosystem Model. Neth. J. Sea Res. 33, 363–379.

Baretta-Bekker, J.G., Baretta, J.W., Hansen, A.S., Riemann, B. 1998. An improved model of carbon and nutrient dynamics in the microbial food web in marine enclosures. Aquat. Microb. Ecol. 14, 91–108.

Baretta-Bekker, J.G., Baretta, J.W., Ebenhöh, W., 1997. Microbial dynamics in the marine ecosystem model ERSEM II with decoupled carbon assimilation and nutrient uptake. J. Sea Res. 38, 195–211 (this issue).

Behrenfeld, M.J., Falkowski, P.G., 1997. Photosynthetic rates derived from satellite-based chlorophyll concentration. Limnol. Oceanogr. 42, 1–20.

Blackford, J.C., Radford, P.J., 1995. A structure and methodology for marine ecosystem modelling. Neth. J. Sea Res. 33, 247–260.

Bratbak, C., Thingstad, T.F., 1985. Phytoplankton–bacteria interactions. Mar. Ecol. Prog. Ser. 25, 23–30.

Daneri, G., 1992. Comparison between in vitro and in situ estimates of primary production within two tracked water bodies. Arch. Hydrobiol. Beih. 37, 101–109.

Dobson, F.W., Smith, S.P., 1988. Bulk model of solar radiation at the sea. Q. J. R. Meteorol. Soc. 114, 165–182.

Droop, M.R., 1974. The nutrient status of algal cells in continuous culture. J. Mar. Biol. Ass. UK 54, 825–855.

Jassby, A.D., Platt, T., 1976. Mathematical formulation of the relationship between photosynthesis and light for phytoplankton. Limnol. Oceanogr. 21, 540–547.

Joint, I., Pomroy, A., 1993. Phytoplankton biomass and production in the southern North Sea. Mar. Ecol. Prog. Ser. 99, 169–182.

Kirk, J.T.O., 1983. Light and Photosynthesis in Aquatic Ecosystems. Cambridge University Press, Cambridge, 401 pp.

Klepper, O., Peters, J.C.H., Van de Kamer, J.P.G., Eilers, P., 1988. The calculation of primary production in an estuary. A model that incorporates the dynamic response of algae, vertical mixing and basin morphology. In: Marani, A. (Ed.), Advances in Environmental Modelling. Elsevier, Amsterdam, pp. 373–394.

Legendre, L., Rassoulzadegan, F., 1995. Plankton and nutrient dynamics in marine waters. Ophelia 41, 153–172.

Lenhart, H.J., Radach, G., Backhaus, J.O., Pohlmann, T., 1995. Simulations of the North Sea circulation, its variability and its implementations as hydrodynamic forcing in ERSEM. Neth. J. Sea Res. 33, 271–299.

McGillicuddy, D.J., 1995. One dimensional numerical simulation of primary production: Lagrangian and Eulerian formulation. J. Plankt. Res. 17, 405–412.

Nyholm, N., 1977. Kinetics of nitrogen-limited algal growth. Prog. Wat. Tech. 8, 347–358.

Nyholm, N., 1978. A mathematical model for growth of phytoplankton. Mitt. Int. Verein. Theor. Angew. Limnol. 21, 193–206.

Radach, G., Pätsch, J., 1997. Climatological annual cycles of nutrients and chlorophyll in the North Sea. J. Sea Res. 38, 231–248 (this issue).

Ruardij, P., Baretta, J.W., Baretta-Bekker, J.G., 1995. SESAME, Software Environment for Simulation and Analysis of Marine Ecosystems in general and for spatially resolved ecosystems in particular. Neth. J. Sea Res. 33, 261–270.

Steele, J.H., 1962. Environmental control of photosynthesis in the sea. Limnol. Oceanogr. 7, 137–150.

Steele, J.H., 1974. The Structure of Marine Ecosystems. Harvard University Press, Cambridge, MA, 128 pp.

Taylor, A.H., Joint, I., 1990. A steady-state analysis of the 'microbial loop' in stratified systems. Mar. Ecol. Prog. Ser. 59, 1–17.

Tett, P., Edwards, A., Jones, K., 1986. A model for the growth of shelf-sea phytoplankton in summer. Estuar. Coast. Shelf Sci. 23, 641–672.

Thingstad, T.F., Rassoulzadegan, F., 1995. Nutrient limitations, microbial food webs, and 'biological C-pumps': suggested interactions in P-limited Mediterranean. Mar. Ecol. Prog. Ser. 117, 299–306.

Varela, R.A., Cruzado, A., Gabaldón, J.E., 1995. Modelling primary production in the North Sea using the European Regional Seas Ecosystem Model. Neth. J. Sea Res. 33, 337–361.